The Asymmetric Trimeric Architecture of [2Fe-2S] IscU: Implications for its Scaffolding during Iron-Sulfur Cluster Biosynthesis*

Yoshimitsu Shimomura[1], Kei Wada[1], Keiichi Fukuyama[1], and Yasuhiro Takahashi[2]*

*Corresponding author

Running Title: Trimeric IscU carrying one [2Fe-2S] cluster

[1]Department of Biological Sciences, Graduate School of Science, Osaka University, Toyonaka, Osaka 560-0043, Japan, [2]Division of Life Science, Graduate School of Science and Engineering, Saitama University, Saitama 338-8570, Japan.

Address correspondence to: Yasuhiro Takahashi, Division of Life Science, Graduate School of Science and Engineering, Saitama University, Saitama 338-8570, Japan. Phone: +81-48-858-3399, Fax: +81-48-858-3384, Email: ytaka@molbiol.saitama-u.ac.jp

Summary

IscU is a key component of ISC machinery and is involved in biogenesis of iron-sulfur (Fe-S) proteins. IscU serves as a scaffold for assembly of a nascent Fe-S cluster, prior to its delivery to an apo-protein. Here we report the first crystal structure of IscU with a bound [2Fe-2S] cluster from the hyperthermophilic bacterium *Aquifex aeolicus*, determined at a resolution of 2.3 Å, using multi-wavelength anomalous diffraction of the cluster. The holo-IscU formed a novel asymmetric trimer that harbored only one [2Fe-2S] cluster. One iron atom of the cluster was coordinate by Sγ atom of Cys36 and Nε of His106, and the other by Sγ atoms of Cys63 and Cys107 on the surface of just one of the protomers. However, the cluster was buried inside the trimer between the neighboring protomers. The three protomers were conformationally distinct from each other, and associated around a non-crystallographic pseudo-three-fold axis. The three flexible loop regions carrying the ligand-binding residues (Cys36, Cys63, His106, and Cys107), and the N-terminal α1 helices were positioned at the interfaces and underwent substantial conformational rearrangement, which stabilized the association of the asymmetric trimer. This unique trimeric *Aa* holo-IscU architecture was clearly distinct from other known monomeric apo-IscU/SufU structures, indicating that asymmetric trimer organization, as well as its association/dissociation, would be involved in the scaffolding function of IscU.

Keywords: Fe-S cluster; biosynthesis; ISC machinery; scaffold; x-ray crystallography

Introduction

Proteins with iron-sulfur (Fe-S) cofactors participate in a wide variety of biological processes including redox and non-redox reactions, and regulation of gene expression.[1-5]

A critical step in their maturation is the biogenesis of their Fe-S clusters, which serve as their active centers. It is now known from genetic and biochemical studies that Fe-S protein maturation is orchestrated by several distinct enzymatic systems *in vivo*, called ISC, NIF, SUF and CIA.[6-10] IscU and NifU are highly conserved scaffold proteins that play central roles in the ISC and NIF systems, respectively.[6] SufU is another homologous protein that is encoded by the *suf*-related operons of several bacteria, including *Thermotoga maritima*.[6,9] These IscU-type proteins can accommodate the assembly of a labile Fe-S cluster by *in vitro* chemical reconstitution, or by enzyme-mediated reconstitution using a cysteine desulfurase (NifS, IscS and SufS) that catalyzes sulfur abstraction from the cysteine substrate.[11-19] These preformed clusters can then be transferred from IscU to Fe-S apo-proteins.[16-19] Therefore IscU-type proteins are thought to serve as molecular scaffolds for the *de novo* synthesis of Fe-S clusters, as suggested by *in vivo* ^{55}Fe radiolabelling experiments of Isu1, a yeast homolog of IscU.[20] In addition, both the ATP-dependent Hsp70 chaperone HscA and its cognate J-type co-chaperone HscB interact with IscU, stimulating HscA ATPase activity and facilitating transfer of the cluster from IscU to an apo-protein.[21-24] However, the mechanistic details of this interaction remain unknown.

The structures of the monomeric IscU apo-form from *Haemophilus influenzae* (*Hi*)[25] and *Mus musculus* (*Mm*), and of SufU from *Bacillus subtilis* (*Bs*) and *Streptococcus pyogenes* (*Sp*)[26] have so far been determined. These structures contain a highly conserved $\alpha+\beta$ globular core architecture, but intriguingly the conformations of the N-terminal segments are quite variable. The three invariant and functionally essential cysteine residues are located on a solvent-accessible surface, on which a zinc ion is coordinated. The additional ligand for this zinc ion is an invariant aspartate (Asp42 in *Sp* SufU) or a well-conserved histidine residue (His105 in *Hi* IscU). Although this zinc-bound structure

is thought to be the putative assembly site for the nascent Fe-S cluster, its coordination scheme and the holo-IscU oligomeric state have been a matter of debate.[14-16,27-29]

We have recently found that IscU from the hyperthermophilic bacterium *Aquifex aeolicus* (*Aa*) harbors a relatively stable [2Fe-2S] cluster, and that a D38A mutation further increased its stability.[30] Here we have determined the crystal structure of the [2Fe-2S] cluster-bound *Aa* IscU-D38A holo-form. In marked contrast to the structures of the apo-IscU/SufU monomers, *Aa* holo-IscU forms an asymmetric trimer in which only one [2Fe-2S] cluster is accommodated. The functional significance of this unique trimeric assembly, as well as its disassembly, is discussed in light of the scaffolding function of IscU, during Fe-S cluster biosynthesis.

RESULTS

The Overall Structure

The crystal structure of the *Aa* IscU-D38A holo-form was determined at 2.3 Å resolution, by multi-wavelength anomalous diffraction (MAD) method, utilizing anomalous dispersion of the Fe atoms in the Fe-S cluster. Structural analysis established that *Aa* IscU forms an asymmetric homotrimer, in which only one subunit (termed protomer B) binds to the [2Fe-2S] cluster. In solution, *Aa* holo-IscU also exists as a trimer with a substoichiometric [2Fe-2S] cluster.[30] This trimer is held together by a number of polar and non-polar interactions, with 1,898 $Å^2$ of the overall surface area buried at the interfaces. The three protomers are related by a pseudo-three-fold-symmetry and come together in a triangular, propeller-like structure, with a radius and height of ~40 and 27 Å, respectively (Fig. 1a). Each protomer is folded into a similar α+β structure that has a rigid core made up of three anti-parallel β-sheets (β1-β3) and five bundled helices (α2-α6) (Fig. 1b). The α1 helix and loops L2, L4 and L7 are conformationally flexible and are involved in the

interprotomer interaction within the trimer (see below). Additionally, a long 12-residue L1-loop crosses over the molecular surface and connects between the α1 helix and the α+β core. *Aa* IscU has a longer C-terminal extension (28-residues) than *Escherichia coli* (*Ec*) IscU. In this region, a unique, short α-helix (α6) and an intramolecular disulfide bond (between Cys31 and Cys138) exist among the three protomers, while the C-terminal regions are disordered after Cys138.

The [2Fe-2S] Cluster Environment

Two Bijvoet difference Fourier maps calculated from the "Sulfur" and "Peak" data unambiguously located the individual sulfur and iron atoms, respectively, within the cluster. Since the respective Δf" values of the sulfur and iron atoms were 0.83 and 0.55 at λ= 1.9074 Å, the sulfur peaks were higher than the iron peaks in the "Sulfur" map. These maps indicate that the cluster has two iron and two sulfur atoms in the form of [2Fe-2S] (Fig. 2a). The cluster is located on the surface of protomer B, which has three Cys residues ($Cys36_B$, $Cys63_B$, and $Cys107_B$; subscripts indicate protomer A, B, or C) and one His residue ($His106_B$) that covalently bind the iron atoms in the cluster, with bond-distances of 2.2-2.3 Å (Fig. 2a). $Cys36_B$ and $Cys63_B$ originate from the $L2_B$ and $L4_B$ loops, respectively, whereas $His106_B$ and $Cys107_B$ lie in the N-terminal region of helix $\alpha5_B$ (Fig. 1b). The 3Cys+1His coordination seen here is unusual among [2Fe-2S] containing proteins, although recent structural studies of mitoNEET, a mitochondrial outer membrane protein with unknown function, indicate its [2Fe-2S] cluster is also coordinated by 3Cys+1His residues.[31-33] However, IscU employs the Nε atom of $His106_B$ for its ligation, unlike mitoNEET, which uses the histidyl Nδ atom. Notably, $His106_B$ is solvent-accessible, which suggests that protonation of this ligand may control the stability of the [2Fe-2S] cluster. The role of the 3Cys+1His residues in cluster coordination fits

with previous *in vivo* studies, in which an Ala-substitution for either one of these residues led to the functional loss of *Azotobacter vinelandii* (*Av*) IscU.[34] Spectroscopic characterization of *in vitro* reconstituted *Av* holo-IscU also suggested cysteine and partial noncysteinyl ligation.[15] On the other hand, the asymmetric trimer structure is incompatible with the previously proposed IscU dimer model, in which one interfacial Fe-S cluster forms a bridge between two molecules.[14] The present structure unequivocally demonstrates that the [2Fe-2S] cluster on the surface of protomer B is covered by, but not ligated to, the N-terminal $\alpha 1_A$ helix of the neighboring protomer (Fig. 2b).

In addition to the 3Cys+1His ligand residues, other residues in this region may also be involved in IscU scaffolding. In the present study, Asp38 of *Aa* IscU was replaced by an Ala residue, which stabilized the [2Fe-2S] cluster.[30] The Cβ atom of the $D38A_B$ methyl group is close (4.3 Å) to one of the sulfur atoms of the cluster (Fig. 2b), suggesting that this Asp residue controls the lability of the cluster via direct interaction. Asp38 is strictly conserved in IscU, SufU, and NifU, and its mutation to Ala abolished the function of *Av* IscU *in vivo*.[34] Candidate residues for coordinating Fe^{2+}, Fe^{3+}, or different forms of the Fe-S clusters are also found around the [2Fe-2S] cluster. These include the side chains of $Asn33_B$ (Oδ), $Ser65_B$ (Oγ), $Asn6_A$ (Nδ) and $Glu7_A$ (Oε), which are close to the cluster (5.5, 5.5, 3.9 and 5.1 Å, respectively) (Fig. 2b). Asn6, Glu7 and Asn33 are not well conserved amongst IscU sequences, whereas Ser65 is almost invariant, suggesting a functional role for this residue. In the NMR structure of *Hi* apo-IscU, Lys103 is close to the Zn-binding site,[25] whereas the side chain of the corresponding residue ($Lys104_B$) of *Aa* IscU is flipped around, with its Nε atom 9.8 Å away from the [2Fe-2S] cluster.

The Interprotomer Interactions Involved in Trimer Association

The asymmetric trimer is held together by heterologous interactions between the

protomers around a central pseudo-three-fold-axis, which primarily involve the N-terminal α1 helix and the L2, L4 and L7 loops of the three protomers. The N-terminal segment of protomer A and its $\alpha1_A$ helix interact with the $L2_B$, $L4_B$ and $L7_B$ loops, as well as $His106_B$ and $Cys107_B$ of $\alpha5_B$ helix, thereby almost completely covering the [2Fe-2S] cluster on the surface of protomer B (Figs. 1a and 2b). In turn, the other side of the $\alpha1_A$ helix associates with protomer C (N terminal segment, $\alpha1_C$ helix, and $L7_C$ loop), and also with the α+β core of protomer A ($\alpha2_A$ and $\alpha4_A$ helices and $L7_A$ loop). Hence, the $\alpha1_A$ helix is anchored near the center of the trimer and packed tightly within the three protomers (Fig. 1a). The $\alpha1_B$ helix is shorter than $\alpha1_A$ by three residues and is sandwiched between the $L7_C$ loop and the α+β core of protomer B. The N-terminal region of protomer C (encompassing the $\alpha1_C$ helix and the $L1_C$ loop) interacts with the $\alpha1_A$ helix, the $L2_A$, $L4_A$ and $L7_A$ loops, and the α+β core of protomer C.

The structures of the cores of the three protomers are similar to one another (Fig. 3a), but we observed notable differences between their N-terminal regions and their L2, L4 and L7 loops (Fig. 3b). These differences are partially due to the coordination of the [2Fe-2S] cluster in protomer B. The N-terminal region of helix $\alpha5_B$ is stable (because $Cys107_B$ and $His106_B$ serve as ligands for the cluster) and is about two helical turns longer than those in other protomers (Figs. 1b and 3a). Significant conformational changes are also induced by the interprotomer interactions, which are most evident in the N-terminal region (Met1-Leu14); helix $\alpha1_A$ is about one turn longer than either the $\alpha1_B$ or $\alpha1_C$ helices, and their preceding N-terminal segments protrude at different angles with respect to each other. The structural alterations in the L7 loops are also a consequence of these heterologous interprotomer interactions, loop $L7_C$ is tightly sandwiched between the $\alpha1_A$ and $\alpha1_B$ helices, whereas loop $L7_A$ interacts only with the $\alpha1_C$ helix and loop $L7_B$ with fewer residues ($Phe3_A$ and $Tyr5_C$). It is noteworthy that the structurally altered regions in protomers A, B

and C fit to these interprotomer interfaces (Figs. 3c and 4a). These observations demonstrate that IscU has considerable structural flexibility and also indicate that the oligomerization of the three protomers involves a number of "induced-fit" interactions.

Structural Comparison with Apo-IscU/SufU

So far, the four characterized IscU and SufU structures represent the monomeric apo-forms of these proteins, with zinc ions bound by their three invariant Cys residues and one His/Asp residue in place of their Fe-S clusters. These residues correspond to Cys36, Cys63, Cys107, and His106/Asp38 of *Aa* IscU, respectively. *Aa* IscU protomers A, B and C share a high structural similarity to those of *Hi* and *Mm* IscU, and their superposition yields rmsd values between 1.37 and 1.69 Å (over 80-104 Cα atoms). Except for the *Aa* IscU C-terminal extension, the α+β cores of these IscUs are folded in virtually identical conformations, with their secondary structural elements deviating only slightly in length (Fig. 5). This reflects their ~50% sequence identity and their high frequency of conserved amino acid substitutions (Fig. 3c). However, most of the differences in their structures lie in their N-terminal regions. In contrast to how the α1 helix and L1 loop are wrapped outside of the core domains of *Aa* IscU, the corresponding *Hi* IscU N-terminal regions are disordered and entirely detached from the other parts of the protein. This difference most likely results from the disassembly of the oligomeric form (discussed below).

The structure of *Aa* IscU is less like the structures of *Sp* and *Bs* SufU, with rmsd values ranging from 1.42 to 2.03 Å for the 76-101 Cα atoms. *Sp* and *Bs* SufU each have a well-ordered N-terminal α1 helix that is longer than the α1 helix of *Aa* IscU, and is tilted at a different angle (Fig. 5). Moreover, notable differences are observed between their α+β core structures. For example, two short α helices (α3 and α4) present in *Aa* IscU are fused to make one long helix in the SufU structures. In addition, the L7 loops of SufU

have a long insertion (17-18 amino acids), which forms one or two helices in the *Bs* or *Sp* SufU, respectively. The flexible L7 loops, of the individual *Aa* IscU protomers, undergo large conformational changes and play major roles in stabilizing the trimer association. Thus, it is unlikely that *Sp* and *Bs* SufU form similar trimeric structures, unless their helices are at least partially unfolded.

DISCUSSION

The most striking aspects of *Aa* holo-IscU structure are its asymmetric architecture and the way in which only one [2Fe-2S] cluster is accommodated in the trimer. This cluster is buried at the interface between protomers A and B, and their association with protomer C further stabilizes this interaction (Figs. 1a and 6). The N-terminal α1 helices and the L2, L4 and L7 loops are conformationally shifted, thereby allowing the asymmetric association to occur (Figs. 3 and 4a). The α1 helix, which is disordered in the *Hi* apo-IscU monomer,[25] is stabilized within the trimer and serves like "glue", holding the structure together by participating in numerous polar and nonpolar interactions. Consistent with this role, *in vivo* function of *Ec* IscU is abolished by truncation of only two N-terminal residues (corresponding to Glu4-Tyr5 in *Aa* IscU, Y.T., unpublished data). These observations, together with the high degree of sequence conservation along the interprotomer interface (Figs. 3c and 4b), suggest that a similar oligomeric architecture is also plausible upon Fe-S cluster assembly for IscU of other organisms. In contrast, variations in the oligomeric state and the Fe-S clusters have so far been reported. For instance, the Fe-S cluster of *Schizosaccharomyces pombe* IscU was reconstituted *in vitro* from Fe^{3+} and S^{2-}, which resulted in a dimer carrying two [2Fe-2S] clusters.[16] *Av* IscU was reported to have one [2Fe-2S] cluster per dimer[14] that can rearrange to two [2Fe-2S] clusters or, with reductive coupling, to one [4Fe-4S] cluster per dimer.[15,35] In addition, a monomeric [2Fe-2S] state

was demonstrated for human IscU.[27] Therefore, an intriguing question is whether the trimeric form of *Aa* IscU is the special case, or IscU undergoes conversion of the oligomeric structures with the Fe-S clusters varying in number or type.

The as-isolated *Aa* IscU holo-form was a trimer in solution[30] as observed in crystals, and *in vitro* reconstitution of the cluster from Fe^{3+} and S^{2-} did not improve the Fe-S cluster content (K.W., unpublished). Thus, the trimeric state carrying only one [2Fe-2S] cluster shown in this study should represent the thermodynamically stable conformation rather than the byproducts resulting from the overproduction in a foreign host or from the partial deterioration during purification and crystallization. Accordingly, the present structure is most likely to indicate a 'locked' state with the Fe-S cluster stabilized by the D38A substitution. Even if the trimeric association is a unique feature of this thermostable *Aa* IscU, the cluster organization and metal coordinating ligands revealed in this study are relevant to understanding the biological Fe-S cluster formation. Further studies will be required to explore the discrepancies in oligomeric state of holo-IscU from different organisms as well as the structural plasticity that is potentially involved in the function of IscU (discussed below).

The present structure is presumably implicated as the conformation that occurs after the initial cluster assembly. Since most of the ligand-binding residues (3Cys+1His) in this trimeric structure are not exposed to the surface (except $Cys36_C$, $Cys107_A$, and $His106_A$), this form of IscU will not directly interact with the sulfur donor (IscS) and iron donor (yet to be clarified). These potential ligand-binding residues of protomers A and C in the trimer are incompetent for the accommodation of the Fe-S cluster without gross changes in tertiary and quaternary structures. In this context, it is noteworthy that *Aa* IscU apo-form adopts the monomeric and dimeric forms,[30] suggesting that these forms provide the actual scaffold site that is competent for the *de novo* Fe-S cluster assembly. Based on these

findings, it seems possible that apo-IscU monomer and/or dimer accepts iron and sulfur atoms from the donor proteins and then builds them into a [2Fe-2S] cluster, and this leads to the association of the asymmetric trimer (Fig. 7). This trimeric structure also suggests that a cooperative interaction between the IscU molecules is likely involved at this early stage of cluster formation.

The extensive nature of the interprotomer interactions, which stabilize the trimer, suggests that the [2Fe-2S] cluster is stably accommodated at the interface and thereby protected from degradation. In contrast, subsequent cluster transfer from IscU to a target apo-protein should involve dissociation of the trimer, which would allow the buried cluster to be exposed on the protomer B surface (Fig. 6). Although the HscA/HscB chaperone system may be attractive candidate that controls the dissociation, it is difficult to envision from the structure how such interactions occur. The *Aa* holo-IscU structure shown here indicates that both the asymmetric trimer and its association/dissociation are the necessary features that allow IscU to function as an Fe-S scaffold. This structure will aid in unraveling the molecular process of Fe-S cluster biosynthesis and provide a rational platform for exploring the interactions between IscU and the other components of the ISC machinery.

Materials and Methods

X-ray Data Collection of *Aa* IscU-D38A Crystals

Details of *A. aeolicus* IscU-D38A expression, purification, and crystallization were described previously.[30] Briefly, $P2_12_12$ crystals of *Aa* IscU-D38A with unit-cell dimensions of a = 72.9, b = 122.1, c = 62.1 Å were grown from a solution containing ammonium sulfate, LiCl, and NaCl by handing-drop vapor diffusion in an anaerobic chamber. These crystals were soaked for a few seconds in a cryoprotectant solution

containing 1.6 M ammonium sulfate, 0.5 M LiCl and 20% glycerol and then flash-cooled at 100 K. Four sets of X-ray diffraction data were collected at 100 K with an ADSC Quantum 315 X-ray CCD detector using synchrotron radiation at the BL41XU station of SPring-8 (Hyogo, Japan). Three data sets were collected around the iron K edge (peak, 1.7407 Å; edge, 1.7423 Å; remote, 1.6947 Å) for phasing by multi-wavelength anomalous scattering of the iron atoms present in the Fe-S cluster and a high-resolution data set at λ = 1.5000 Å for structural refinement. All diffraction data sets were measured from one crystal and processed and scaled with the HKL2000 program suite.[36] An additional data set was collected at λ = 1.9074 Å ($\Delta f_s'' = 0.83$) to locate the sulfur atoms of the Fe-S cluster and the cysteine residues.

Determination of *Aa* IscU-D38A Structure

Initial clue of the phase information was obtained by single anomalous diffraction using the peak data set. A Bijvoet difference Patterson map located one Fe-S cluster, from which the phase angles were calculated. The Bijvoet difference Fourier map at 2.4 Å resolution was then calculated based on these phase angles and showed one elongated peak, indicating that the densities of the two closely positioned Fe atoms were overlapped. These two Fe sites were used for MAD analysis. The overall figure of merit was 0.45 in the 50 - 2.4 Å resolution range. The MAD phase angles derived from the two Fe sites were combined with the structure amplitude from the high-resolution data. Then, solvent flattening and phase extension to 2.3 Å resolution were performed using CNS.[37] Automated tracing of the polypeptide chain using SOLVE/RESOLVE[38] placed 189 of the total 471 residues (the three *Aa* IscU-D38A molecules in an asymmetric unit) into 27 fragments. These fragments were then connected manually by the symmetry and/or translation operations, and the subsequent manual model building led to a complete *Aa*

IscU-D38A structure. Several cycles of model refinement and water picking with CNS were followed by manual revision of the model with Xfit[39] performed using the high-resolution data. The sites of the iron and sulfur atoms were confirmed by the Bijvoet difference maps using the data sets collected at λ = 1.7407 Å and λ = 1.9074 Å, respectively. Finally, a [2Fe-2S] cluster was incorporated manually with Xfit, and further refinement was carried out with CNS. Due to the large conformational differences observed between the three protomers, structural models were built and refined independently. The geometry between the [2Fe-2S] cluster and ligands was not restrained during the refinement. The data collection and refinement statistics are summarized in Table 1. Assignment of secondary structure within the models and analysis of the geometry of the final models were performed using PROCHECK.[40] Superposition and rmsd of the structures were calculated using LSQMAN.[41] The interactions between the protomers were analyzed using the Protein-Protein Interaction Server.[42] The phylogenetic conservation of the residues was determined using CONSURF.[43]

Protein Data Bank accession codes

The coordinates and structure factors have been deposited at the RCSB Protein Data Bank under accession code 2Z7E.

Acknowledgments

The synchrotron radiation experiments were performed with the approval of the JASRI (proposal nos. 2005B0984 and 2006A2727). We thank Drs N. Shimizu and M. Kawamoto (Japan Synchrotron Radiation Research Institute) for their aid with data collection at SPring-8.

This study was supported in part by Grants-in-Aid for Scientific Research 17570112

and 18054018 (to Y.T.) and 18770084 (to K.W.), and National Project on Protein Structural and Functional Analyses (to K.F.) from the Ministry of Education, Culture, Sports, Science and Technology of Japan, and also by Research Fellowships of the Japan Society for the Promotion of Science for Young Scientists (to Y.S.).

Footnotes

The abbreviations used are: Fe-S, iron-sulfur; MAD, multi-wavelength anomalous diffraction; *Aa*, *Aquifex aeolicus*; *Hi*, *Haemophilus influenzae*; *Mm*, *Mus musculus*; *Bs*, *Bacillus subtilis*; *Sp*, *Streptococcus pyogenes*; *Ec*, *Escherichia coli*; *Av*, *Azotobacter vinelandii*.

References

1. Beinert, H., Holm, R. H. & Münck, E. (1997). Iron-sulfur clusters: nature's modular, multipurpose structures. *Science*, **277**, 653-659.
2. Johnson, M. K. (1998). Iron-sulfur proteins: new roles for old clusters. *Curr. Opin. Chem. Biol.*, **2**, 173-181.
3. Kiley, P. J. & Beinert, H. (2003). The role of Fe-S proteins in sensing and regulation in bacteria. *Curr. Opin. Microbiol.*, **6**, 181-185.
4. Rees, D. C. & Howard, J. B. (2003). The interface between the biological and inorganic worlds: iron-sulfur metalloclusters. *Science*, **300**, 929-931.
5. Fontecave, M. (2006). Iron-sulfur clusters: ever-expanding roles. *Nat. Chem. Biol.*, **2**, 171-174.
6. Johnson, D. C., Dean, D. R., Smith, A. D. & Johnson, M. K. (2005). Structure, function, and formation of biological iron-sulfur clusters. *Annu. Rev. Biochem.*, **74**, 247-281.
7. Lill, R. & Mühlenhoff, U. (2005). Iron-sulfur-protein biogenesis in eukaryotes. *Trends Biochem. Sci.*, **30**, 133-141.
8. Barras, F., Loiseau, L. & Py, B. (2005). How *Escherichia coli* and *Saccharomyces*

cerevisiae build Fe/S proteins. *Adv. Microb. Physiol.*, **50**, 41-101.

9. Tokumoto, U., Kitamura, S., Fukuyama, K. & Takahashi, Y. (2004). Interchangeability and distinct properties of bacterial Fe-S cluster assembly systems: functional replacement of the *isc* and *suf* operons in *Escherichia coli* with the *nifSU*-like operon from *Helicobacter pylori*. *J. Biochem. (Tokyo)*, **136**, 199-209.
10. Ayala-Castro, C., Saini, A. & Outten, F. W. (2008). Fe-S cluster assembly pathways in bacteria. *Microbiol. Mol. Biol. Rev.*, **72**, 110-125.
11. Smith, A. D., Agar, J. N., Johnson, K. A., Frazzon, J., Amster, I. J., Dean, D. R. & Johnson, M. K. (2001). Sulfur transfer from IscS to IscU: the first step in iron-sulfur cluster biosynthesis. *J. Am. Chem. Soc.*, **123**, 11103-11104.
12. Urbina, H. D., Silberg, J. J., Hoff, K. G. & Vickery, L. E. (2001). Transfer of sulfur from IscS to IscU during Fe/S cluster assembly. *J. Biol. Chem.*, **276**, 44521-44526.
13. Yuvaniyama, P., Agar, J. N., Cash, V. L., Johnson, M. K. & Dean, D. R. (2000). NifS-directed assembly of a transient [2Fe-2S] cluster within the NifU protein. *Proc. Natl. Acad. Sci. USA*, **97**, 599-604.
14. Agar, J. N., Zhang, L., Cash, V. L., Dean, D. R. & Johnson, D. C. (2000). Role of the IscU protein in iron-sulfur cluster biosynthesis: IscS-mediated assembly of a $[Fe_2S_2]$ cluster in IscU. *J. Am. Chem. Soc.*, **122**, 2136-2137.
15. Agar, J. N., Krebs, C., Frazzon, J., Huynh, B. H., Dean, D. R. & Johnson, M. K. (2000). IscU as a scaffold for iron-sulfur cluster biosynthesis: sequential assembly of [2Fe-2S] and [4Fe-4S] clusters in IscU. *Biochemistry*, **39**, 7856-7862.
16. Wu, G., Mansy, S. S., Wu Sp, S. P., Surerus, K. K., Foster, M. W. & Cowan, J. A. (2002). Characterization of an iron-sulfur cluster assembly protein (ISU1) from *Schizosaccharomyces pombe*. *Biochemistry*, **41**, 5024-5032.
17. Mansy, S. S., Wu, G., Surerus, K. K. & Cowan, J. A. (2002). Iron-sulfur cluster biosynthesis. *Thermatoga maritima* IscU is a structured iron-sulfur cluster assembly protein. *J. Biol. Chem.*, **277**, 21397-21404.
18. Wu, S. P., Wu, G., Surerus, K. K. & Cowan, J. A. (2002). Iron-sulfur cluster biosynthesis. Kinetic analysis of [2Fe-2S] cluster transfer from holo ISU to apo Fd: role of redox chemistry and a conserved aspartate. *Biochemistry*, **41**, 8876-8885.
19. Dos Santos, P. C., Smith, A. D., Frazzon, J., Cash, V. L., Johnson, M. K. & Dean, D. R. (2004). Iron-sulfur cluster assembly: NifU-directed activation of the nitrogenase

Fe protein. *J. Biol. Chem.*, **279**, 19705-19711.

20. Mühlenhoff, U., Gerber, J., Richhardt, N. & Lill, R. (2003). Components involved in assembly and dislocation of iron-sulfur clusters on the scaffold protein Isu1p. *EMBO J*, **22**, 4815-4825.
21. Chandramouli, K. & Johnson, M. K. (2006). HscA and HscB stimulate [2Fe-2S] cluster transfer from IscU to apoferredoxin in an ATP-dependent reaction. *Biochemistry*, **45**, 11087-11095.
22. Craig, E. A. & Marszalek, J. (2002). A specialized mitochondrial molecular chaperone system: a role in formation of Fe/S centers. *Cell. Mol. Life Sci.*, **59**, 1658-1665.
23. Tokumoto, U., Nomura, S., Minami, Y., Mihara, H., Kato, S., Kurihara, T., Esaki, N., Kanazawa, H., Matsubara, H. & Takahashi, Y. (2002). Network of protein-protein interactions among iron-sulfur cluster assembly proteins in *Escherichia coli*. *J. Biochem. (Tokyo)*, **131**, 713-719.
24. Vickery, L. E. & Cupp-Vickery, J. R. (2007). Molecular chaperones HscA/Ssq1 and HscB/Jac1 and their roles in iron-sulfur protein maturation. *Crit. Rev. Biochem. Mol. Biol.*, **42**, 95-111.
25. Ramelot, T. A., Cort, J. R., Goldsmith-Fischman, S., Kornhaber, G. J., Xiao, R., Shastry, R., Acton, T. B., Honig, B., Montelione, G. T. & Kennedy, M. A. (2004). Solution NMR structure of the iron-sulfur cluster assembly protein U (IscU) with zinc bound at the active site. *J. Mol. Biol.*, **344**, 567-583.
26. Liu, J., Oganesyan, N., Shin, D. H., Jancarik, J., Yokota, H., Kim, R. & Kim, S. H. (2005). Structural characterization of an iron-sulfur cluster assembly protein IscU in a zinc-bound form. *Proteins*, **59**, 875-881.
27. Foster, M. W., Mansy, S. S., Hwang, J., Penner-Hahn, J. E., Surerus, K. K. & Cowan, J. A. (2000). A mutant human IscU protein containts a stable $[2Fe\text{-}2S]^{2+}$ center of possible functional significance. *J. Am. Chem. Soc.*, **122**, 6805-6806.
28. Adinolfi, S., Rizzo, F., Masino, L., Nair, M., Martin, S. R., Pastore, A. & Temussi, P. A. (2004). Bacterial IscU is a well folded and functional single domain protein. *Eur. J. Biochem.*, **271**, 2093-2100.
29. Mansy, S. S. & Cowan, J. A. (2004). Iron-sulfur cluster biosynthesis: toward an understanding of cellular machinery and molecular mechanism. *Acc. Chem. Res.*, **37**,

719-725.

30. Shimomura, Y., Kamikubo, H., Nishi, Y., Masako, T., Kataoka, M., Kobayashi, Y., Fukuyama, K. & Takahashi, Y. (2007). Characterization and crystallization of an IscU-type scaffold protein with bound [2Fe-2S] cluster from the hyperthermophile, *Aquifex aeolicus*. *J. Biochem. (Tokyo)*, **142**, 577-586.
31. Paddock, M. L., Wiley, S. E., Axelrod, H. L., Cohen, A. E., Roy, M., Abresch, E. C., Capraro, D., Murphy, A. N., Nechushtai, R., Dixon, J. E. & Jennings, P. A. (2007). MitoNEET is a uniquely folded 2Fe-2S outer mitochondrial membrane protein stabilized by pioglitazone. *Proc. Natl. Acad. Sci. USA*, **104**, 14342-14347.
32. Lin, J., Zhou, T., Ye, K. & Wang, J. (2007). Crystal structure of human mitoNEET reveals distinct groups of iron sulfur proteins. *Proc. Natl. Acad. Sci. USA*, **104**, 14640-14645.
33. Hou, X., Liu, R., Ross, S., Smart, E. J., Zhu, H. & Gong, W. (2007). Crystallographic Studies of Human MitoNEET. *J. Biol. Chem.*, **282**, 33242-33246.
34. Johnson, D. C., Unciuleac, M. C. & Dean, D. R. (2006). Controlled expression and functional analysis of iron-sulfur cluster biosynthetic components within *Azotobacter vinelandii*. *J. Bacteriol.*, **188**, 7551-7561.
35. Chandramouli, K., Unciuleac, M. C., Naik, S., Dean, D. R., Huynh, B. H. & Johnson, M. K. (2007). Formation and properties of [4Fe-4S] clusters on the IscU scaffold protein. *Biochemistry*, **46**, 6804-6811.
36. Otwinowski, Z. & Minor, W. (1997). Processing of X-ray diffraction data collected in oscillation mode. *Methods Enzymol.*, **276**, 307-326.
37. Brünger, A. T., Adams, P. D., Clore, G. M., DeLano, W. L., Gros, P., Grosse-Kunstleve, R. W., Jiang, J. S., Kuszewski, J., Nilges, M., Pannu, N. S., Read, R. J., Rice, L. M., Simonson, T. & Warren, G. L. (1998). Crystallography & NMR system: A new software suite for macromolecular structure determination. *Acta Crystallogr.*, **A54**, 905-921.
38. Terwilliger, T. C. (2003). Automated main-chain model building by template matching and iterative fragment extension. *Acta Crystallogr.*, **D59**, 38-44.
39. McRee, D. E. (1999). XtalView/Xfit--A versatile program for manipulating atomic coordinates and electron density. *J. Struct. Biol.*, **125**, 156-165.
40. Laskowski, R. A., MacArthur, M. W., Moss, D. S. & Thornton, J. M. (1993).

PROCHECK: a program to check the stereochemical quality of protein structures. *J. Appl. Cryst.*, **26**, 283-291.

41. Kleywegt, J. M. & Jones, T. A. (1994). A super position. *ESF/CCP4 Newsletter*, **31**, 9-14.

42. Jones, S. & Thornton, J. M. (1996). Principles of Protein-Protein Interactions Derived From Structural Studies. *Proc. Natl. Acad. Sci. USA*, **93**, 13-20.

43. Glaser, F., Pupko, T., Paz, I., Bell, R. E., Bechor-Shental, D., Martz, E. & Ben-Tal, N. (2003). ConSurf: identification of functional regions in proteins by surface-mapping of phylogenetic information. *Bioinformatics*, **19**, 163-164.

44. Kakuta, Y., Horio, T., Takahashi, Y. & Fukuyama, K. (2001). Crystal structure of *Escherichia coli* Fdx, an adrenodoxin-type ferredoxin involved in the assembly of iron-sulfur clusters. *Biochemistry*, **40**, 11007-11012.

Figure legends

Fig. 1. The crystal structure of *Aa* holo-IscU. (a) The overall structure of the asymmetric trimer. The conformationally distinct protomers A, B and C are colored in pink, green, and blue, respectively. The [2Fe-2S] cluster is shown (red rhombus). (b) The structure of protomer B and its [2Fe-2S] cluster. The α helices (green, α1-α6), β strands (orange, β1-β3), loop regions (magenta, L1-L8) and iron (cyan) and sulfur (yellow) atoms are depicted.

Fig. 2. The coordination environment of the [2Fe-2S] cluster. (a) Bijvoet difference maps around the [2Fe-2S] cluster were calculated from the Bijvoet differences of the "Sulfur" (red, contoured at 6.0 σ) and "Peak" (blue, contoured at 25.0 σ) data sets, which contain large anomalous scattering signals from the sulfur and iron atoms, respectively. The phases were derived from the refined model. The [2Fe-2S] cluster and the ligated residues

are shown in a stick model: oxygen (red), nitrogen (blue), sulfur (yellow) and iron (cyan). (b) A close-up view of the residues around the [2Fe-2S] cluster. The [2Fe-2S] cluster is coordinated by $Cys36_B$, $Cys63_B$, $His106_B$, and $Cys107_B$ of protomer B (green) and is overlaid by the α1 helix of protomer A (pink).

Fig. 3. Conformational deviation in the three protomers. (a) A superposition of the Cα traces of protomers A, B, and C using LSQMAN.[41] Rmsd values are 0.90 Å for 124 Cα atoms between protomers A and B, 0.82 Å for 120 Cα atoms between A and C, and 0.89 Å for 118 Cα atoms between B and C. The segments with marked differences in conformation are colored as follows: cyan, Ser2-Phe13; green, Gly32-Asp38; blue, Thr60-Ala66; magenta, Ile93, Phe94, Leu97-Leu110; yellow, Glu23, Gln126, Gly127, Tyr139. The [2Fe-2S] cluster in protomer B is shown as red rhombus. (b) Graph compares the pairwise distances between the corresponding Cα atoms of protomers A and B (green trace), A and C (red trace), B and C (blue trace). The residues involved in the Fe-S cluster coordination in protomer B are indicated by triangles (Δ). (c) Alignment of multiple IscU, NifU and SufU sequences. The highlights indicate invariant (red) and conserved (blue) residues and the numbers refer to the *A. aeolicus* IscU sequence. Only the N-terminal domain of NifU, which is homologous to IscU/SufU, is shown. The secondary structures of the *Aa* IscU protomers A, B and C are shown above the alignment. The color bars on the secondary structure indicate the residues involved in the intermolecular interaction with protomer A (pink), B (green), and C (blue). The conformationally altered regions shown in (a) and (b) are boxed (red). The residues involved in the Fe-S cluster coordination are indicated by inverted triangles (∇) above the alignment.

Fig. 4. Representation of the trimeric *Aa* IscU structure. (a) Structural rearrangement is involved in the interprotomer interactions. The conformationally altered regions among the three protomers are color-coded (as in Fig. 3a). (b) Sphere models show the distribution of highly conserved (purple) and variable (cyan) residues on the trimer surface. The phylogenetic conservation of the residues was determined using CONSURF analysis of 88 IscU sequences.[43]

Fig. 5. Structural comparison among the IscU/SufU homologs. Ribbon diagrams are shown for (*upper row*) *Aa* IscU protomers A, B, and C and (*bottom row*) *H. influenzae* (*Hi*) (PDB ID: 1R9P) and *M. musculus* (*Mm*) IscU (PDB: 1WFZ) and *S. pyogenes* (*Sp*) (PDB: 1SU0) and *B. subtilis* (*Bs*) SufU (PDB: 2AZH). The *Aa* IscU α3 (Ile82-Leu86) and α4 helices (Tyr90-Glu96 and their corresponding regions) are shown in green, and the L7 loops are shown in magenta. The SufU specific insertions are denoted in cyan, Gln101-Ala119 in *Sp* SufU and Lys102-Ser120 in *Bs* SufU. The N-terminal region of *Hi* IscU was disordered in the NMR structure and omitted from the model. In the *Mm* IscU structure, the N-terminal amino acids were truncated and replaced with unrelated sequence during the plasmid construction.

Fig. 6. Sequestration of the [2Fe-2S] cluster in trimeric IscU. (*upper panel*) The [2Fe-2S] cluster is buried between the neighboring protomers in the asymmetric trimer. (*lower panel*) The [2Fe-2S] cluster is exposed on the surface of protomer B. Iron and sulfur atoms are colored in cyan and yellow, and the protomers A, B and C are in pink, green, and blue, respectively.

Fig. 7. Model for the role of an asymmetric IscU trimer during Fe-S cluster biosynthesis. Monomeric and dimeric apo-IscU exist in an equilibrium.[30] Sulfur and iron atoms are

donated to IscU from IscS and IscX/IcsA/CyaY, respectively. Electrons are probably donated from Fdx, an adrenodoxin-type ferredoxin.[44] Upon assembly of a nascent [2Fe-2S] cluster, a holo-IscU molecule associates with two apo-IscU molecules to form an asymmetric trimer, sequestering the cluster at the interface. The interaction with the HscA-HscB chaperone system may induce dissociation of the trimeric structure, thereby providing a trigger for cluster release. This model is proposed based on the structure of *Aa* IscU and the biochemical studies on the ISC components from other bacteria and mitochondria. It should be noted that *A. aeolicus* does not possess the genes for several components (IscX, CyaY, and HscB).

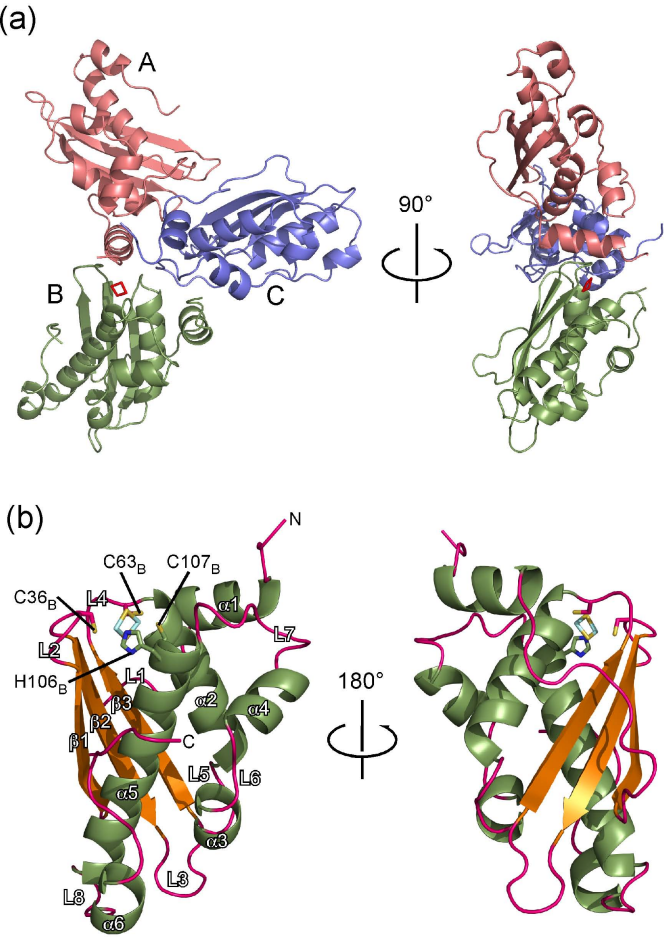
(a)
A
B
C
90°
(b)
N
C63B
C107B
C36B
L4
α1
L7
L2
L1
H106B
β3
α2
α4
β2
β1
C
L5
L6
α5
α3
L3
L8
α6
180°

Figure 1

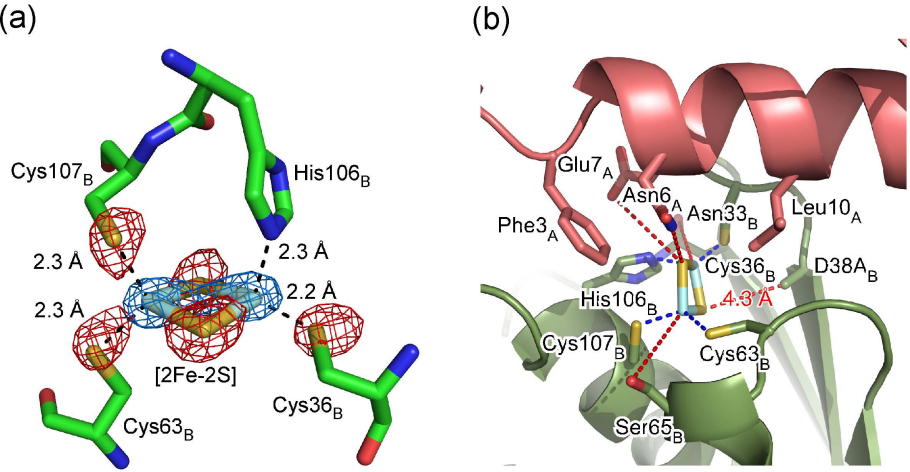
(a)
Cys107B
His106B
2.3 Å
2.3 Å
2.2 Å
2.3 Å
[2Fe-2S]
Cys63B
Cys36B
(b)
Glu7A
Asn6A
Asn33B
Leu10A
Phe3A
Cys36B
D38AB
His106B
4.3 Å
Cys107B
Cys63B
Ser65B

Figure 2

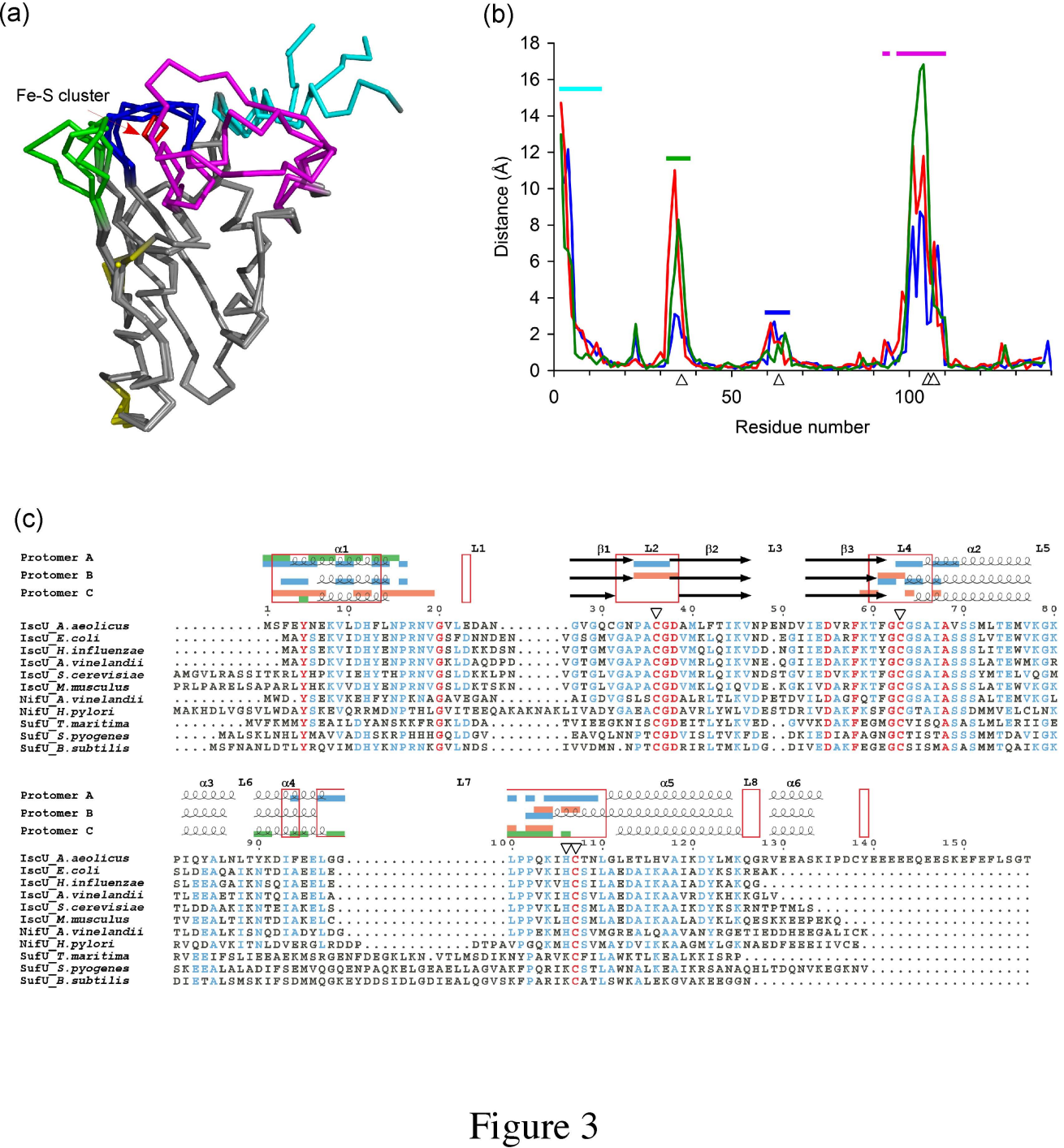
(a)
Fe-S cluster
(b)
Distance (Å)
Residue number
(c)
Protomer A
Protomer B
Protomer C
IscU_A.aeolicus
IscU_E.coli
IscU_H.influenzae
IscU_A.vinelandii
IscU_S.cerevisiae
IscU_M.musculus
NifU_A.vinelandii
NifU_H.pylori
SufU_T.maritima
SufU_S.pyogenes
SufU_B.subtilis

Figure 3

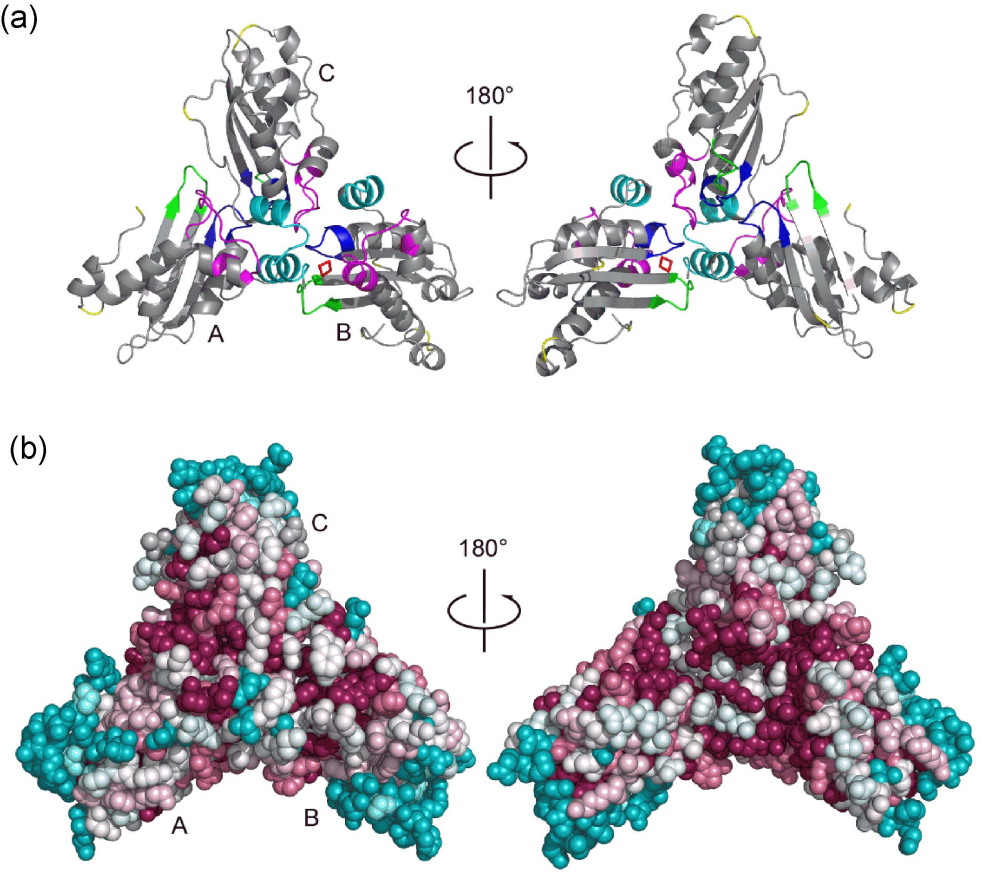

Figure 4

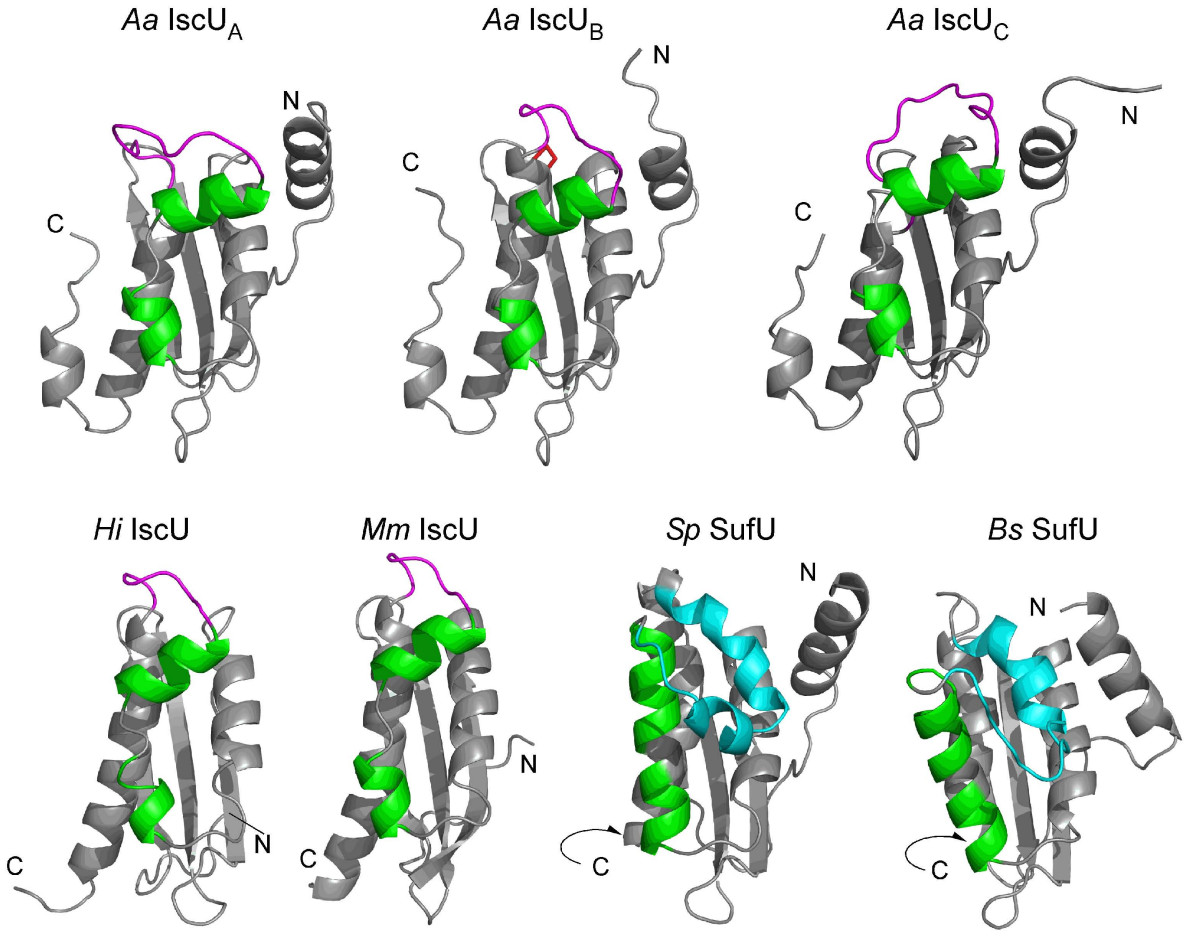
Aa IscU$_A$
N
C
Aa IscU$_B$
N
C
Aa IscU$_C$
N
C
Hi IscU
N
C
Mm IscU
N
C
Sp SufU
N
C
Bs SufU
N
C

Figure 5

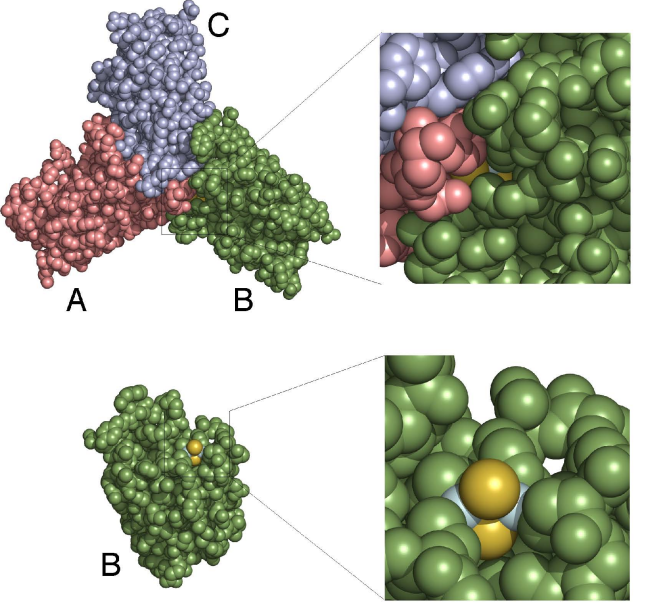

Figure 6

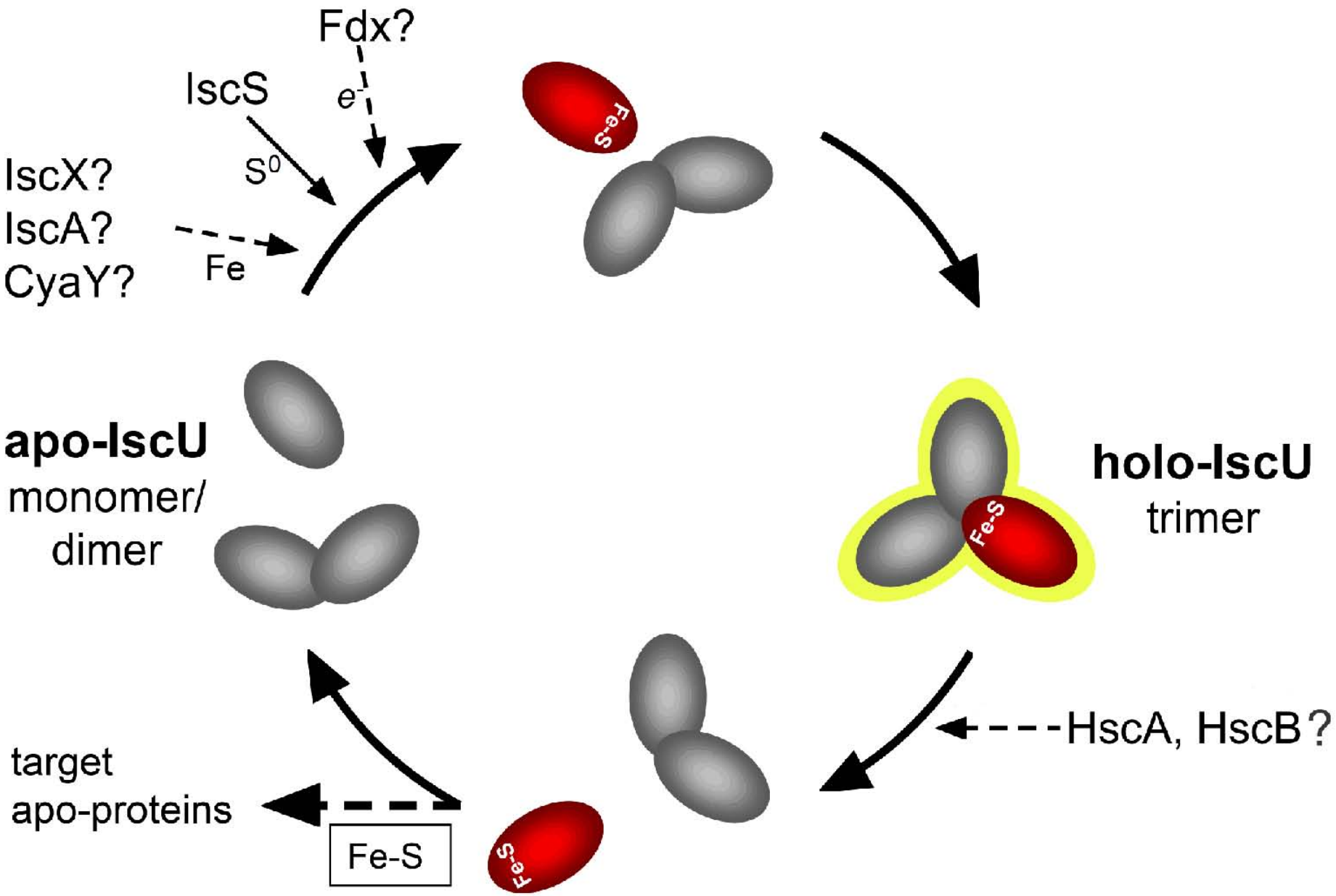
Fdx?
IscS
e-
S0
IscX?
IscA?
CyaY?
Fe
Fe-S
apo-IscU
monomer/
dimer
holo-IscU
trimer
Fe-S
HscA, HscB?
target
apo-proteins
Fe-S
Fe-S

Figure 7

Table 1. Data collection and refinement statistics

	High-resolution	Peak	Edge	Remote	Sulfur
Crystallographic data					
Wavelength, Å	1.5000	1.7407	1.7423	1.6947	1.9074
Cell parameters, Å			a = 72.9, b = 122.1, c = 62.1		
Resolution range,* Å	50 – 2.30 (2.38 – 2.30)	50 – 2.35 (2.43 – 2.35)	50 – 2.40 (2.49 – 2.40)	50 – 2.40 (2.49 – 2.40)	30 – 2.50 (2.59 – 2.50)
Measured reflections	260156	163193	155874	163098	191114
Unique reflections	24481	23025	21679	22106	19584
Redundancy*	10.6 (6.7)	7.1 (4.1)	7.2 (6.1)	7.4 (6.1)	9.8 (5.8)
Completeness,* %	96.8 (79.1)	96.8 (76.5)	97.1 (78.8)	98.7 (89.7)	98.2 (90.1)
R_{sym},*[†] %	7.9 (23.9)	7.4 (26.0)	7.9 (27.3)	7.6 (27.2)	5.8 (35.0)
Refinement statistics					
R-factor / R_{free},[‡§] %	22.5 / 25.2				
No. of solvent molecules					
Water	162				
SO_4^{2-}	4				
RMSD from ideal values					
Bond length, Å	0.007				
Bond angle, °	1.3				
Average B-factor, Å^2	49.9				
Ramachandran plot					
Most favored, %	88.4				
Additionally allowed, %	10.5				
Generously allowed, %	1.1				

* Values in parentheses are for the outermost shells.

† $R_{sym} = \Sigma_{hkl}\Sigma_i|I_i(hkl) - \langle I(hkl)\rangle|/ \Sigma_{hkl}\Sigma_i I_i(hkl)$, where $\langle I(hkl)\rangle$ is the average intensity over equivalent reflections.

‡ R-factor $= \Sigma||F_{obs}(hkl)| - |F_{calc}(hkl)||/ \Sigma|F_{obs}(hkl)|$.

§ R_{free} is the R-factor computed for the test set of reflections that were omitted from the refinement process.